Acta Biochim Biophys Sin 2023, 55(3): 484–497
https://doi.org/10.3724/abbs.2023023
Advance Access Publication Date: 3 March 2023
Original Article

Original Article

lncRNA ELFN1-AS1 upregulates TRIM29 by suppressing miR-211-3p to promote gastric cancer progression

Jinxi Huang[1], Weiwei Yuan[1], Beibei Chen[2], Gaofeng Li[1], and Xiaobing Chen[2,*]

[1]Department of General Surgery, the Affiliated Cancer Hospital of Zhengzhou University, Zhengzhou 450003, China, and [2]Department of Oncology, the Affiliated Cancer Hospital of Zhengzhou University, Zhengzhou 450003, China
*Correspondence address. Tel: +86-13937100233; E-mail: xiaobingchen89@163.com

Received 5 September 2022 Accepted 26 October 2022

Abstract

Long noncoding RNA (lncRNA) extracellular leucine rich repeat and fibronectin type III domain containing 1-antisense RNA 1 (ELFN1-AS1) has been found to be upregulated in various tumors. However, the biological functions of ELFN1-AS1 in gastric cancer (GC) are not entirely understood. In the present study, the expression levels of ELFN1-AS1, miR-211-3p, and TRIM29 are determined using reverse transcription-quantitative PCR. Subsequently, CCK8, EdU, and colony formation assays are performed to determine GC cell vitality. The migratory and invasive capabilities of GC cells are further evaluated using transwell invasion and cell scratch assays. Western blot analysis is performed to quantify the levels of proteins associated with GC cell apoptosis and epithelialmesenchymal transition (EMT). The competing endogenous RNA (ceRNA) activity of ELFN1-AS1 on TRIM29 through miR-211-3p is confirmed by pull-down, RIP, and luciferase reporter assays. Our study proves that ELFN1-AS1 and TRIM29 are highly expressed in GC tissues. *ELFN1-AS1* silencing inhibits GC cell proliferation, migration, invasion and EMT, and induces cell apoptosis. Rescue experiments reveal that the oncogenicity of ELFN1-AS1 is modulated by acting as a sponge for miR-211-3p, thereby increasing the expression of the target gene of miR-211-3p, *TRIM29*. In summary, ELFN1-AS1 maintains GC cell tumorigenicity via the ELFN1-AS1/miR-211-3p/TRIM29 axis, indicating that this axis can be directed for GC treatment in the future.

Key words ELFN1-AS1, TRIM29, migration, invasion, proliferation, interplay

Introduction

Gastric cancer (GC) is a frequently diagnosed gastrointestinal cancer, with more than one million new cases and approximately 770,000 mortalities in 2020 worldwide [1]. Currently, surgical debulking in combination with radiotherapy and chemotherapy can improve the clinical outcomes for GC patients. However, patients with metastatic GC miss the optimal treatment window because of late diagnoses [2]. According to epidemiological studies, genetics and ethnicity, along with *Helicobacter pylori* infection, diet, and lifestyle, are associated with GC incidence and mortality burden [3]. Therefore, the discovery of novel effective targets in GC occurrence and progression is required for clinical application.

Long noncoding RNAs (lncRNAs) are noncoding transcripts greater than 200 nucleotides. Various studies have demonstrated that lncRNAs are commonly dysregulated and act as tumor suppressors or oncogenes in GC. lncRNAs predominantly regulate gene expression, thereby influencing cancer genesis and progression [4]. For example, the lncRNA MT1JP is downregulated in GC, increasing the malignant phenotypes of GC cells and decreasing the survival of GC patients, thus acting as a tumor-suppressive lncRNA [5]. Ectopically expressed lncRNA NMRAL2P is speculated to induce DNA methyltransferase 3 activity, which reduces the expression of acyl-CoA thioesterase 7 through methylation, indicating a tumor-suppressive role of NMRAL2P in GC progression [6]. In contrast, the lncRNA ANRIL promotes GC progression by regulating downstream genes and thus acts as an oncogene. ANRIL is upregulated in GC tissues, whereas ten-eleven translocation protein 2, which binds to the promoter of *ANRIL* and regulates its expression, is downregulated [7,8]. Since lncRNAs constitute a major part of the human genome, gaining a better understanding of how they function in GC is crucial.

Currently, extracellular leucine rich repeat and fibronectin type III domain containing 1-antisense RNA 1 (ELFN1-AS1) has been

found to be highly regulated and play a protumorigenic role in various cancers, such as esophageal, colorectal, ovarian, and pancreatic cancers [9–13]. Additionally, ELFN1-AS1 deficiency was found to impair cancer cell proliferation, migration, invasion, and epithelial-mesenchymal transition (EMT), thereby limiting cancer progression. Although the expression of ELFN1-AS1 is enhanced in GC samples according to an analysis using the GEPIA database, its expression and role in GC have not been previously reported.

Tripartite motif-containing 29 (TRIM29) belonging to the TRIM protein family is characterized by multiple zinc finger motifs and a leucine zipper motif. It functions as a putative scaffold or adaptor in DNA double-strand break repair. Therefore, TRIM29 dysregulation is suggested to be associated with various pathological disorders, including tumors [14]. Recent studies have reported that TRIM29 plays either a pro-oncogenic or tumor-suppressive role in different types of cancers. For example, TRIM29 deficiency in hepatocellular carcinoma cells elicits the Wnt/β-catenin signaling pathway, consequently promoting malignant phenotypes of cancer cells and accelerating cancer growth [15]. In contrast, TRIM29 is over-expressed in lung squamous cell carcinoma, and high-TRIM29 patients exhibit the shortest survival rate [16]. In GC, high TRIM29 expression is closely associated with clinical pathological characteristics and an unfavorable prognosis [17]. Furthermore, TRIM29 has previously been defined as an oncoprotein that exhibits proliferative, migratory, and invasive characteristics *in vitro* via hyperactivation of the Wnt/β-catenin signaling pathway [18]. However, the specific regulatory mechanism of TRIM29 in GC remains unclear.

In the present study, an unregulated lncRNA, ELFN1-AS1, was detected in GC tissues using GEPIA database analysis. Subsequently, we performed cellular functional assays, which demonstrated the protumorigenic feature of ELFN1-AS1 with clinical significance. We found that ELFN1-AS1 acts as a competing endogenous RNA (ceRNA) for miR-211-3p, enhances the transcriptional activity of TRIM29, and promotes GC cell progression. Our findings provide a better understanding of how lncRNAs function during GC malignancy and a new direction for investigating effective targets in GC diagnosis and treatment.

Materials and Methods

Bioinformatics analysis

GEPIA database (http://gepia.cancer-pku.cn/index.html) was used to show the levels of TRIM29 and ELFN1-AS1 in GC samples and normal samples. Meanwhile, Kaplan-Meier Plotter (KMplot, http://kmplot.com/analysis/) was used to show the association between the prognosis of GC and the expression of TRIM29 and ELFN1-AS1. Finally, the miRNAs binding to ELFN1-AS1 was predicted by miRDB (https://mirdb.org/), whereas the miRNAs targeting TRIM29 was predicted by TargetScan (https://www.targetscan.org/vert_71/) and miRWalk (https://mirdb.org/).

Clinical specimens

GC tissues ($n=40$) and paired adjacent noncancerous tissues ($n=40$) were obtained from patients in our hospital after obtaining informed consent. This study was approved by the Ethics Committee of our hospital. The patient data are shown in Table 1. All surgically resected tissues were collected and immediately stored at −80°C for RNA isolation.

Table 1. Baseline characteristics of 40 patients with gastric cancer

Characteristic	Number (n=40)
Age (years), *n* (%)	
≤60	27 (67.5)
>60	13 (32.5)
Gender, *n* (%)	
Male	25 (62.5)
Female	15 (37.5)
Lymph node metastasis, *n* (%)	
Negative	19 (47.5)
Positive	21 (52.5)
Invasion depth, *n* (%)	
T1 + T2	13 (32.6)
T3 + T4	27 (67.5)
TNM stage, *n* (%)	
I	11 (27.5)
II	5 (12.5)
III	24 (60.0)
Tumor size, *n* (%)	
≤4 cm	23 (57.5)
>4 cm	17 (42.5)
Tumor differentiation, *n* (%)	
High and medium	11 (27.5)
Low and none	29 (72.5)

Reverse transcription-quantitative PCR (RT-qPCR)

A PureLink RNA Mini kit (Thermo Fisher, Waltham, USA) was used for RNA extraction. RNA quality was spectrophotometrically determined using the 260/280 ratio before performing reverse transcription of 1 μg RNA using the QuantiTect Reverse Transcription kit (Qiagen, Shanghai, China). RT-qPCR was performed to examine mRNA expression. *U6* or *GAPDH* was used as the internal control, and the $2^{-\Delta\Delta Ct}$ method was used to analyze the data. The primer sequences used in the study are listed in Table 2.

Nuclear-cytoplasmic fractionation

A PARIS kit (Invitrogen, Carlsbad, USA) was used to determine the subcellular localization of ELFN1-AS1 according to the manufac-

Table 2. The sequences of PCR primers used in this study

Gene	Primer sequence
lnc-ELFN1-AS1	Forward: 5′-AAAAGTTGACGCCGCATTCT-3′
	Reverse: 5′-GAGAATGGATTGTGGGTGCC-3′
TRIM29	Forward: 5′-CACCGCCACTCATTGCCCGCGAAC-3′
	Reverse: 5′-AAACGTTCGCGGGCAATGAGTGGC-3′
miR-211-3p	Forward: 5′-ACACTCCAGCTGGGGCAGGGACAG CAAAG-3′
	Reverse: 5′-CTCAACTGGTGTCGTGGAGTCGGCA ATTCAGTTGAGTCCCCACG-3′
GAPDH	Forward: 5′-CCAGGTGGTCTCCTCTGA-3′
	Reverse: 5′-GCTGTAGCCAAATCGTTGT-3′
U6	Forward: 5′-CTCGCTTCGGCAGCACA-3′
	Reverse: 5′-AACGCTTCACGAATTTGCGT-3′

turer's instructions. Briefly, 1×10^6 AGS and MKN74 cells were collected, and RNA was isolated from the nucleus and cytoplasm using 500 μL Cell Disruption buffer and centrifugation at 500 *g* and 4°C. Finally, qRT-PCR was used to identify the location of ELFN1-AS1, with *U6* and *GAPDH* as nuclear and cytoplasmic controls, respectively.

Cell culture and transfection

GC cell lines (HGC-27, AGS, MKN74, and GTL-16) and the normal human gastric epithelial cell line GES-1 were purchased from ATCC (Manassas, USA). Cells were maintained in RPMI-1640 (HGC-27, MKN74, and GES-1) or Ham's F-12 (AGS) medium supplemented with 10% fetal bovine serum and antibiotics at 37°C with 5% CO_2.

For transfection, two siRNAs (si-ELFN1-AS1#1 and si-ELFN1-AS1#2), an overexpression vector of ELFN1-AS1 (OE-lnc), miR-211-3p mimic/inhibitor, siRNA-TRIM29, and their negative controls (NC) were purchased from GenePharma (Guangzhou, China). All sequences of siRNAs are listed in Table 3. Then, 100 nM of the aforementioned vectors were transfected or cotransfected into AGS and MKN74 cells (1×10^6) using Lipofectamine 3000 (Invitrogen) according to the manufacturer's instructions. qRT-PCR was performed to assess the transfection efficiency after 48 h.

Droplet digital PCR (ddPCR)

For ELFN1-AS1, TaqMan reaction mix (Applied Biosystems, Waltham, USA) containing 30 ng/20 μL sample cDNA was separated into aqueous droplets in oil using the QX100 Droplet Generator (Bio-Rad, Hercules, USA) and then transferred to a 96-well PCR plate. A two-step thermocycling protocol (95°C × 10 min; 40 cycles of 94°C × 30 s and 60°C × 60 s; and 98°C × 10 min) was developed using Bio-Rad C1000. For miR-211-3p, the miRCURY LNA miRNA PCR assay (Qiagen) was used. The cycling conditions were 95°C for 5 min, 40 cycles (95°C for 30 s and 58°C for 1 min), and 90°C for 5 min. The PCR plate was loaded onto a droplet reader (Bio-Rad), which directly determined the copy number of each gene per μL PCR. Analysis software QuantaSoft 1.7.4 (Bio-Rad) and Poisson statistics were used to calculate droplet concentrations (copies/μL).

Western blot analysis

The cells were lysed using protein lysis buffer. After microcentrifugation, the supernatant was collected, and the protein concentration was analyzed using a BCA kit (Thermo Fisher Scientific). We loaded 20 μg protein (per sample) onto a 10% SDS-PAGE gel, separated them by electrophoresis, and then electrotransferred them to a PVDF membrane. Subsequently, the membrane was blocked with blocking buffer for 1 h at room temperature, followed by incubation with primary antibody at 4°C overnight. The antibodies used in this study were as follows: BAX (cat#: 2772; 1:1000; Cell Signaling, Danvers, USA), Bcl-2 (cat#: AB112; 1:1000; Beyotime, Shanghai, China), E-cadherin (cat#: AF6759; 1:1000; Beyotime), vimentin (cat#: AF1975; 1:1000; Beyotime), and GAPDH (cat#: AF5009; 1:1000; Beyotime). After incubation with the appropriate secondary antibodies for 1 h at room temperature, the blots were detected using ECL (Amersham Biosciences, Piscataway, USA).

Table 3. The sequences of siRNAs used in this study

Name	Sequence
si-ELFN1-AS1#1	5′-GCUUGUGGUUUCUCACAAA-3′
si-ELFN1-AS1#2	5′-CCUUUAAUCUCUUGCUCAA-3′
si-TRIM29	5′-GGGACAAGACTATGCTTTA-3′
si-NC	5′-UUCUCCGAACGUGUCACGUTT-3′
miR-211-3p mimic	5′-GCAGGGACAGCAAAGGGGUGC-3′
Mimic-NC	5′-UUCUCCGAACGUGUCACG-3′
miR-211-3p inhibitor	5′-UACAAAAGGGUAGUGAAAGUA-3′
Inhibitor-NC	5′- UAGAACUUGCAUUGCAACCGG-3′

RIP analysis

An EZ-Magna RIP RNA-binding protein immunoprecipitation kit (Millipore, Billerica, USA) was used to analyze the interaction between ELFN1-AS1 and miR-211-3p. AGS and MKN74 cells (5×10^3) were transfected with 50 pM miR-211-3p or NC. At 48 h post-transfection, the cells were incubated using RIP lysis buffer and treated with magnetic beads conjugated with anti-Ago2 or negative control IgG at 4°C. After 4 h of inoculation, the RIP lysate was incubated with proteinase K and underwent RNA purification for further quantification of ELFN1-AS1 in cells by qRT-PCR [19].

RNA pull-down analysis

AGS and MKN74 cells (5×10^3) were transfected with the 50 pM 3′-biotinylated miR-211-3p mimic (BiomiR-211-3p mimic) or Bio-NC (RiboBio, Guangzhou, China) for 48 h. Cells were harvested after transfection for 48 h and lysed in lysis buffer. The lysate was incubated with streptavidin magnetic beads (Invitrogen) for 10 min. The RNA-binding protein complexes were washed and eluted before RT-qPCR analysis of TRIM29 according to a previous study [20].

Luciferase reporter assay

The recombinant vectors psiCHECK-2-ELFN1-AS1-wild type (WT), psiCHECK-2-ELFN1-AS1-mutant (MUT), psiCHECK-2-TRIM29 3′-UTR-WT, and psiCHECK-2-TRIM29 3′-UTR mutant (MUT) were synthesized by GenePharma (Shanghai, China). The constructed luciferase reporter vectors (100 ng/well) were co-transfected into AGS and MKN74 cells (2×10^5 cells/well) with 50 nM miR-211-3p mimic or mimic-NC. The luciferase activity in total cell lysates was measured 48 h after co-transfection, as described previously [21].

CCK8 assays

CCK8 was used to measure cell viability. Briefly, the transfected cells (1×10^3 cells/well) were seeded in a 96-well plate. Cells were cultured for 24 h, 48 h, 72 h, and 96 h. At the end of each time point, cells were treated with 10 μL CCK8 solution (Beyotime) for 2 h. Finally, the plate was read at 450 nm using a microplate spectrophotometer (ELx800; BioTek, Vermont, USA).

EdU proliferation assay

An EdU Staining Proliferation kit (Abcam) was used to detect the proliferation of GC cells. Briefly, transfected cells (1×10^3 cells/well) were seeded into a 24-well plate and then treated with 50 μM EdU stain for 2 h. Subsequently, the cells were fixed with 4% paraformaldehyde for 15 min before permeabilization with 0.5% Triton X-100. The resulting complex was sequentially stained with DAPI for 30 min before being photographed and counted under a fluorescence microscope (Olympus, Tokyo, Japan).

Colony formation assay

GC cells (1.5×10^3 cells/well) were seeded into 6-well plates and cultured for 14 days. The plates were fixed with 4% paraformaldehyde and stained with 0.02% crystal violet for 15 min. Cell colonies containing > 50 cells were counted and imaged using a scanner.

Scratch wound healing assay

Scratch wound healing assay was performed to test the migration of GC cells. Briefly, AGS and MKN74 cells (4×10^5 cells/well) were incubated in a 12-well plate. After 24 h of growth, a sterile 1 mL pipette tip was used to scratch across the center of the well and the detached cells were removed. The plates were incubated for 24 h. Images of cell morphology at 0 h and 24 h were captured under a microscope (100×), and the gap distance was quantitatively evaluated using ImageJ software.

Cell invasion assay

Cells (5×10^4 cells/well) with serum-free medium were plated into a Chill Millicell insert (Merck KGaA, Munich, Germany) precoated with Matrigel. This insert was positioned in the well of a plate containing DMEM supplemented with 10% FBS as an attractant. After 24 h, the inserts were removed, and noninvasive cells were removed. The lower side of the insert was fixed with 5% glutaraldehyde for 10 min before staining with 1% crystal violet for 20 min. The invaded cells were quantitatively assessed and photographed under a microscope (250×).

Animal experiments

The animal experiments were approved by the Ethics Committee of the Affiliated Cancer Hospital of Zhengzhou University (Zhengzhou, China). The shRNA against ELFN1-AS1 (sh-ELFN1-AS1, the same target as si-lnc) and sh-NC were cloned into the lentiviral vector pLL3.7. Then, AGS cells (1.0×10^7 cells/150 μL PBS) transfected with 5×10^6 TU/mL sh-ELFN1-AS1 or sh-NC were subcutaneously injected into the left inguinal region of male BALB/c athymic nude mice (~4 weeks old, $n = 5$ in each group) purchased from Hunan SJA Laboratory Animals (Changsha, China). Tumor volumes were calculated by the formula: Tumor volume = (length × width^2)/2 and measured every 4 days. After 21 days, the mice were sacrificed, and the tumors were weighed.

Statistical analysis

All *in vitro* assays were conducted in triplicate. The results are shown as the mean ± SD. Statistical evaluation was performed using GraphPad Prism. Comparisons between two groups were conducted using an unpaired Student's *t* test, and the correlation of mRNA expression was examined using the Spearman correlation test. One-way analysis of variance with Bonferroni post hoc analysis was performed for comparisons among multiple groups. $P < 0.05$ was considered statistically significant.

Results

ELFN1-AS1 and miR-211-3p regulate TRIM29 expression and affect GC progression

TRIM29 was significantly upregulated in GC (data obtained from the GEPIA database; Figure 1A) and was significantly associated with poor prognosis in GC patients (data obtained from KMplot; Figure 1B). Similarly, ELFN1-AS1 was upregulated in GC (Figure 1C), which was related to poor overall survival outcomes in GC patients (Figure 1D). To identify a connecting miRNA between ELFN1-AS1 and TRIM29, we predicted the miRNAs that target ELFN1-AS1 (using miRDB) and TRIM29 (using TargetScan and miRWalk). We found five miRNAs that targeted both ELFN1-AS1 and TRIM29 mRNAs (Figure 1E). Finally, miR-211-3p, miR-4447, miR-711-5p, miR-6870-5p, and miR-5698 expressions were detected by RT-qPCR, which revealed that miR-211-3p expression was the lowest in GC tissues (Figure 1F–J). Therefore, miR-211-3p was identified as a sensitive miRNA.

Upregulation of ELFN1-AS1 in GC tissues and cell lines

First, we compared ELFN1-AS1 expression in four widely used GC cell lines (HGC-27, AGS MKN74, and GTL-16) with that in GSE-1 cells. Enhanced expression of ELFN1-AS1 was detected in GC cell lines, especially in AGS and MKN74 cells (Figure 2A). Next, we found that ELFN1-AS1 was highly expressed in 40 GC tissues and 40 noncancerous gastric mucosal tissues by RT-qPCR (Figure 2B) and ddPCR (Supplementary Figure S1A). ELFN1-AS1 expression was substantially elevated in GC tissues. To further investigate the function of ELFN1-AS1 in GC, we analyzed its subcellular localization in AGS and MKN74 cells and found that ELFN1-AS1 was predominantly found in the cytoplasm (Figure 2C), suggesting that ELFN1-AS1 functions as a ceRNA in GC. These data suggest a potential role of ELFN1-AS1 in GC progression. For further analysis, we silenced *ELFN1-AS1* in AGS and MKN74 cells using two siRNAs (si-ELFN1-AS1#1 and si-ELFN1-AS1#2) (Figure 2D).

ELFN1-AS1 silencing impedes GC cell proliferation, migration, invasion, and EMT, activates apoptosis and inhibits tumor growth *in vivo*

CCK8 assays demonstrated that *ELFN1-AS1*-silenced AGS and MKN74 cells had significantly lower proliferative capacity than si-NC-transfected cells (Figure 3A). Reduced proliferation of si-lnc-transfected cells was also observed in the EdU cell proliferation assay (Figure 3B). *ELFN1-AS1* silencing led to a diminished colony formation rate in both cell lines (Figure 3C). The protein levels of apoptosis-related factors Bax and Bcl-2 were detected by western blot analysis. *ELFN1-AS1* silencing upregulated Bax expression and downregulated Bcl-2 expression in AGS and MKN74 cells (Figure 3D).

We also evaluated the migratory and invasive capacities of AGS and MKN74 cells. Quantification of the scratch wound healing assay demonstrated an impaired migration distance of AGS and MKN74 cells (approximately 0.5 fold) when *ELFN1-AS1* was silenced (Figure 4A). Similarly, the Transwell invasion assays showed that *ELFN1-AS1* knockdown significantly reduced the invasion capacity of both GC cell lines compared with that of the NC group (Figure 4B). These *in vitro* findings indicate that ELFN1-AS1 may act as an oncogenic RNA in GC progression. We further investigated whether ELFN1-AS1 influences EMT in GC cells by analyzing two EMT markers, E-cadherin and vimentin. Our results demonstrated that *ELFN1-AS1* silencing significantly increased E-cadherin level but decreased vimentin level in both cell lines, suggesting the inhibition of EMT (Figure 4C).

Additionally, a stable AGS cell line containing sh-ELFN1-AS1 or sh-NC was constructed and subcutaneously injected into nude mice to establish a xenograft tumor model. Tumor volume was significantly lower in the *ELFN1-AS1*-knockdown group than in the control group (Figure 4D). Moreover, when tumor samples were collected 21 days later, the tumor sizes and weights were reduced in

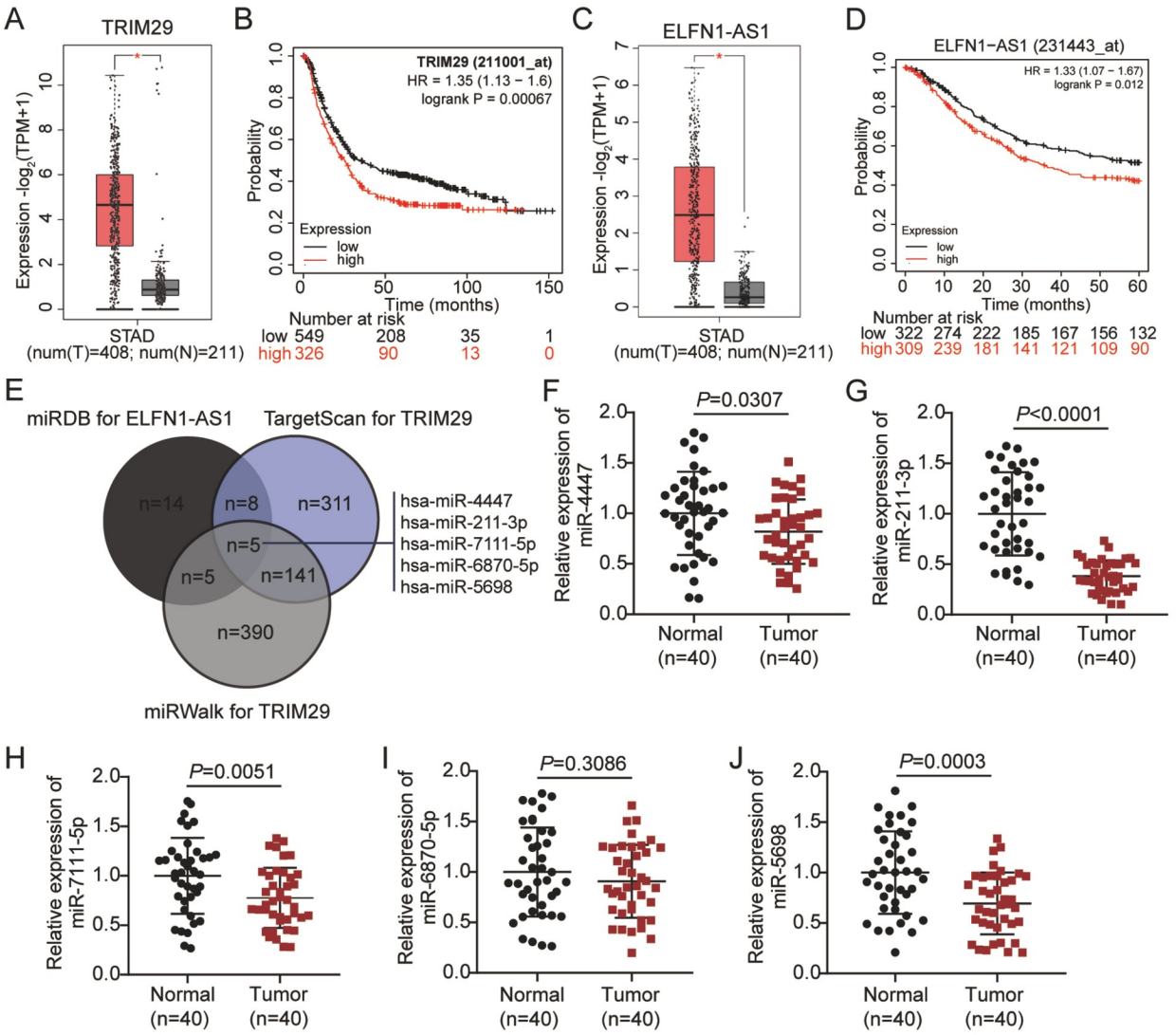

Figure 1. The expression and prognostic significance of ELFN1-AS1 and TRIM29 in GC (A) The expression of TRIM29 in GC. Data are obtained from the GEPIA database. STAD: stomach adenocarcinoma. T: tumor. N: healthy. (B) The overall survival outcome of patients with GC according to the expression level of TRIM29. Data are obtained from KMplot.com. (C) The expression of ELFN1-AS1 in GC. (D) The overall survival outcome of patients with GC according to the expression level of ELFN1-AS1. (E) The intersection between the targets of ELFN1-AS1 and TRIM29 mRNA 3′UTR. The targets for ELFN1-AS1 were predicted using miRDB. The targets for TRIM29 were predicted using TargetScan and miRWalk (3′UTR position and score = 1). (F–J) The expressions of miR-447, miR-211-3p, miR-7111-5p, miR-6870-5p and miR-5698 in GC and adjacent normal samples.

the sh-ELFN1-AS1 group (Figure 4E,F). These *in vivo* findings supported the *in vitro* findings, indicating that *ELFN1-AS1* knockdown reduces GC tumorigenicity.

ELFN1-AS1 functions as a miR-211-3p *sponge* in GC cells

Considering the preferential accumulation of ELFN1-AS1 in the cytoplasm of GC cells, we attempted to elucidate the underlying mechanism of ELFN1-AS1 as a ceRNA in GC progression. miRDB predicted that miR-211-3p had binding sites in the 3′-UTR sequence of *ELFN1-AS1* (Figure 5A). Next, a luciferase reporter assay was conducted to verify whether miR-211-3p physically targets ELFN1-AS1 in GC cells. Two ELFN1-AS1 *Luciferase* reporter vectors were generated: wild-type (WT) and mutant-type ELFN1-AS1 (MUT). Following cotransfection, synthetic miR-211-3p overexpression could reduce the luciferase activity of WT-ELFN1-AS1 group, but it did not change the luciferase activity of MUT-ELFN1-AS1 group (Figure 5B), suggesting that miR-211-3p physically interacts with ELFN1-AS1. This miRNA-mRNA interaction was also confirmed by the RIP assay (Figure 5C), which demonstrated the enrichment of ELFN1-AS1 in the Ago2 group. Absolute quantification of miR-211-3p in tissues showed that the level of miR-211-3p in cancer tissues was lower than that in normal tissues (Supplementary Figure S1B). Additionally, ELFN1-AS1 and miR-211-3p were negatively correlated (Figure 5D and Supplementary Figure S1C). Moreover, we found that miR-211-3p expression was lower in the two GC cell lines than in the GSE-1-cell line as revealed by RT-qPCR (Figure 5E). Since RT-qPCR results showed that the difference in ELFN1-AS1 expression between both sets was significantly low, only one (si-

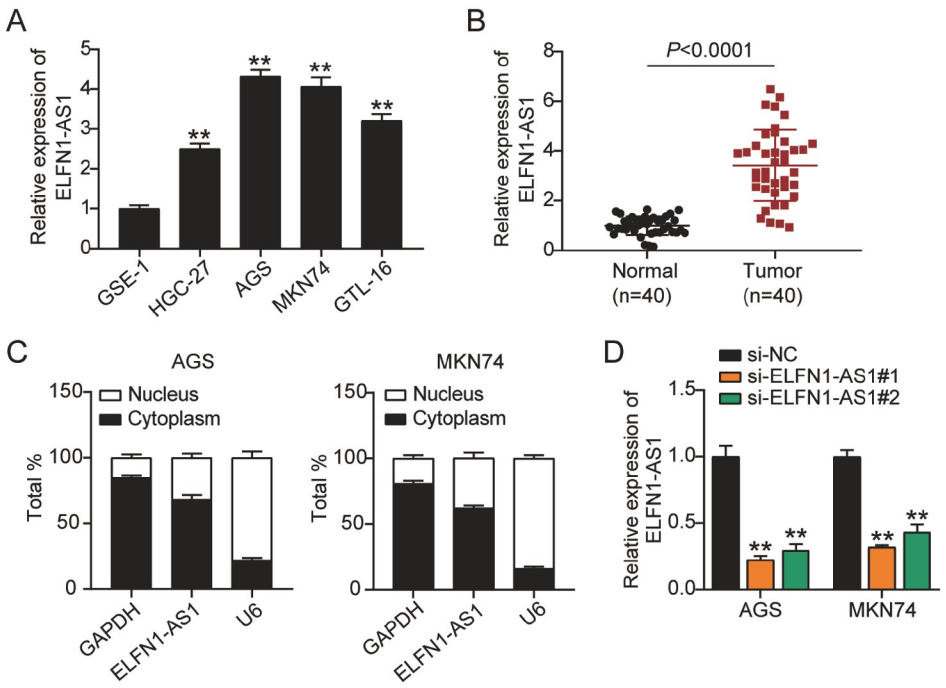

Figure 2. Frequent upregulation of *ELFN1-AS1* in GC tissues and cell lines (A) RT-qPCR analysis of *ELFN1-AS1* expression levels in GC cell lines (HGC-27, AGS, MKN74, and GTL-16) and GSE-1 cells. $^{**}P < 0.001$ vs GSE-1 cells. (B) The expression level of *ELFN1-AS1* was measured in 40 GC tissues and 40 normal tissues. (C) Levels of *ELFN1-AS1* in the nuclear and cytoplasmic fractions of AGS and MKN74 cells. (D) Expression level of *ELFN1-AS1* in AGS and MKN74 cells transfected with si-NC, si-ELFN1-AS1#1 or si-ELFN1-AS1#2. $^{**}P < 0.01$ vs si-NC.

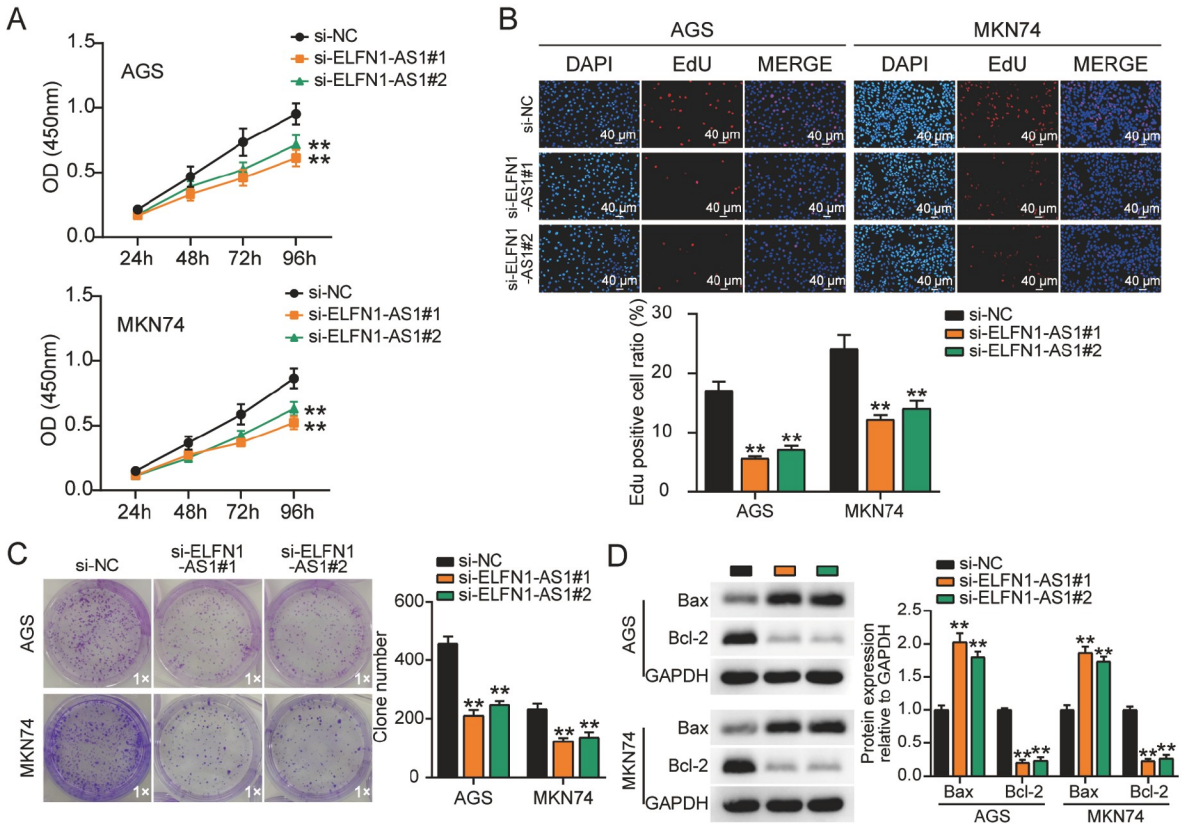

Figure 3. *ELFN1-AS1* silencing impedes proliferation and activates apoptosis in GC cells *in vitro* (A) CCK8 assays assessing the proliferation of si-ELFN1-AS1#1, si-ELFN1-AS1#2 and si-NC AGS and MKN74 cells ($n = 3$). (B) Proliferation of si-ELFN1-AS1#1, si-ELFN1-AS1#2 and si-NC AGS and MKN74 cells measured by EdU cell proliferation assay ($n = 3$). (C) Colony formation assays of AGS and MKN74 cells with ELFN1-AS1 silencing ($n = 3$). (D) The levels of Bax and Bcl-2 were measured by western blot analysis. $^{**}P < 0.01$ vs si-NC.

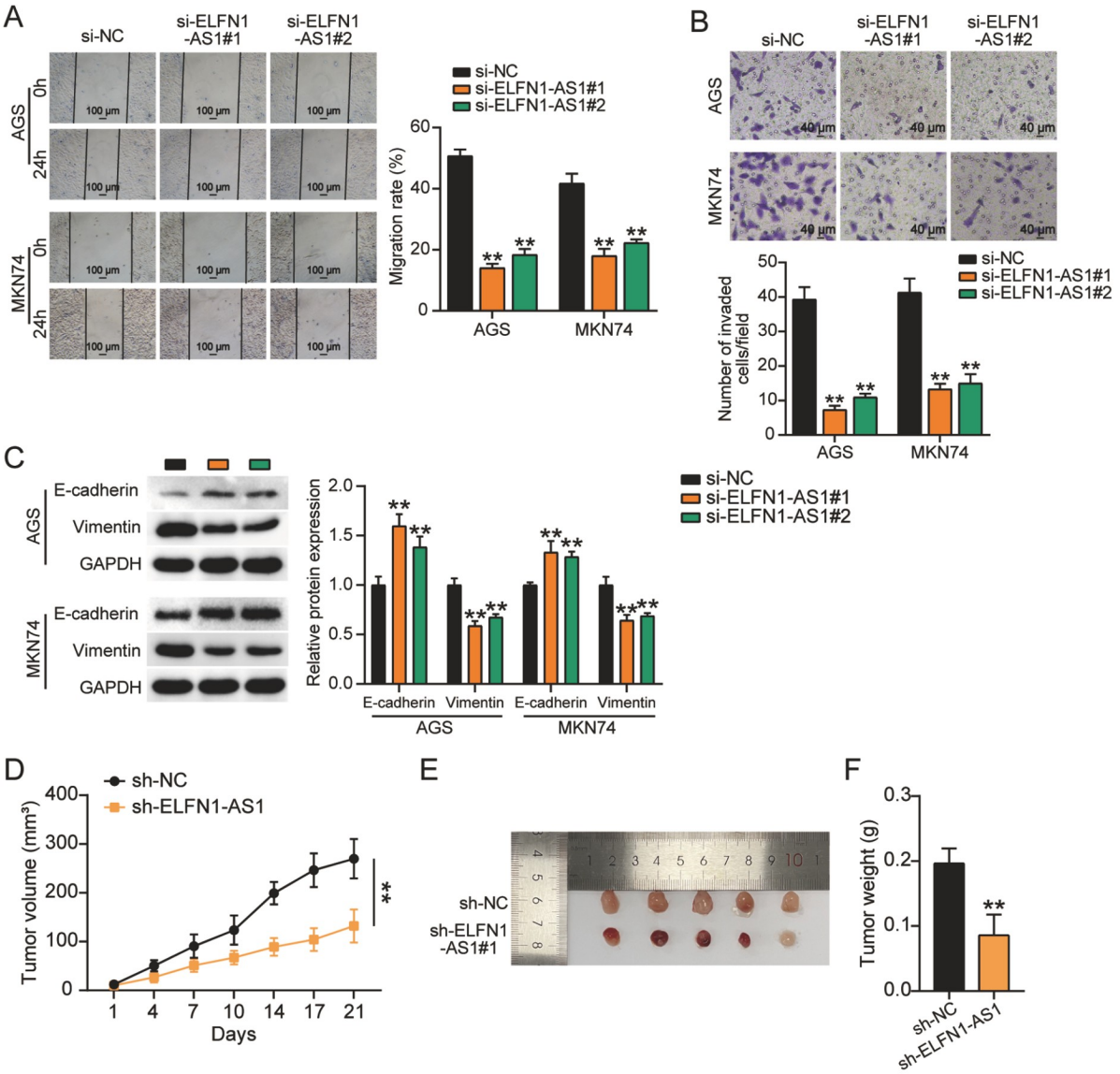

Figure 4. ***ELFN1-AS1*** **silencing impedes the migration and invasion of GC cells** ***in vitro*** **and** ***in vivo*** (A) Wound healing assays of AGS and MKN74 cells with ELFN1-AS1 silencing. (B) Transwell assays of the two GC cell lines with ELFN1-AS1 silencing. (C) The levels of E-cadherin and Vimentin were measured by western blot analysis. (D) Three weeks after treatment, xenograft tumor volumes were recorded. (E) Images of subcutaneous xenograft tumors of AGS cells. (F) The tumor weight of AGS cells is shown. $^{**}P < 0.01$ vs si-NC.

ELFN1-AS1#1) was used for further experiments. We cotransfected si-lncRNA and miR-211-3p inhibitors to validate the inverse correlation between ELFN1-AS1 and miR-211-3p. *ELFN1-AS1* knockdown resulted in a 50% increase in the expression of miR-211-3p, but this effect was cancelled in the two GC cell lines upon transfection with miR-211-3p inhibitor (Figure 5F). Thus, ELFN1-AS1 functions as a ceRNA for miR-211-3p during GC progression.

miR-211-3p inhibitor alleviates the effect of *ELFN1-AS1* knockdown on proliferation, migration, invasion, apoptosis, and EMT of GC cells *in vitro*

Subsequent *in vitro* functional assays were performed to validate the interaction between ELFN1-AS1 and miR-211-3p in GC cells. *ELFN1-AS1* silencing inhibited GC cell viability, whereas miR-211-3p inhibitor treatment promoted the viability of the two GC cell lines. The inhibitory effect of *ELFN1-AS1* silencing on GC cell viability was reversed by the miR-211-3p inhibitor (Figure 6A). The EdU proliferation assay also demonstrated that the addition of the miR-211-3p inhibitor alleviated the inhibitory effect of *ELFN1-AS1* knockdown on cell proliferation (Figure 6B). Similarly, the miR-211-3p inhibitor eliminated the suppressive effect of *ELFN1-AS1* knockdown on the colony formation of AGS and MKN74 cells (Figure 6C). We discovered that miR-211-3p inhibitor treatment decreased Bax expression and increased Bcl-2 expression, which was contrary to what was observed with *ELFN1-AS1* knockdown. However, cotransfection of the miR-211-3p inhibitor with si-ELFN1-AS1 reversed the effects of *ELFN1-AS1* knockdown (Figure 6D).

In addition to modulating GC cell proliferation, the effect of

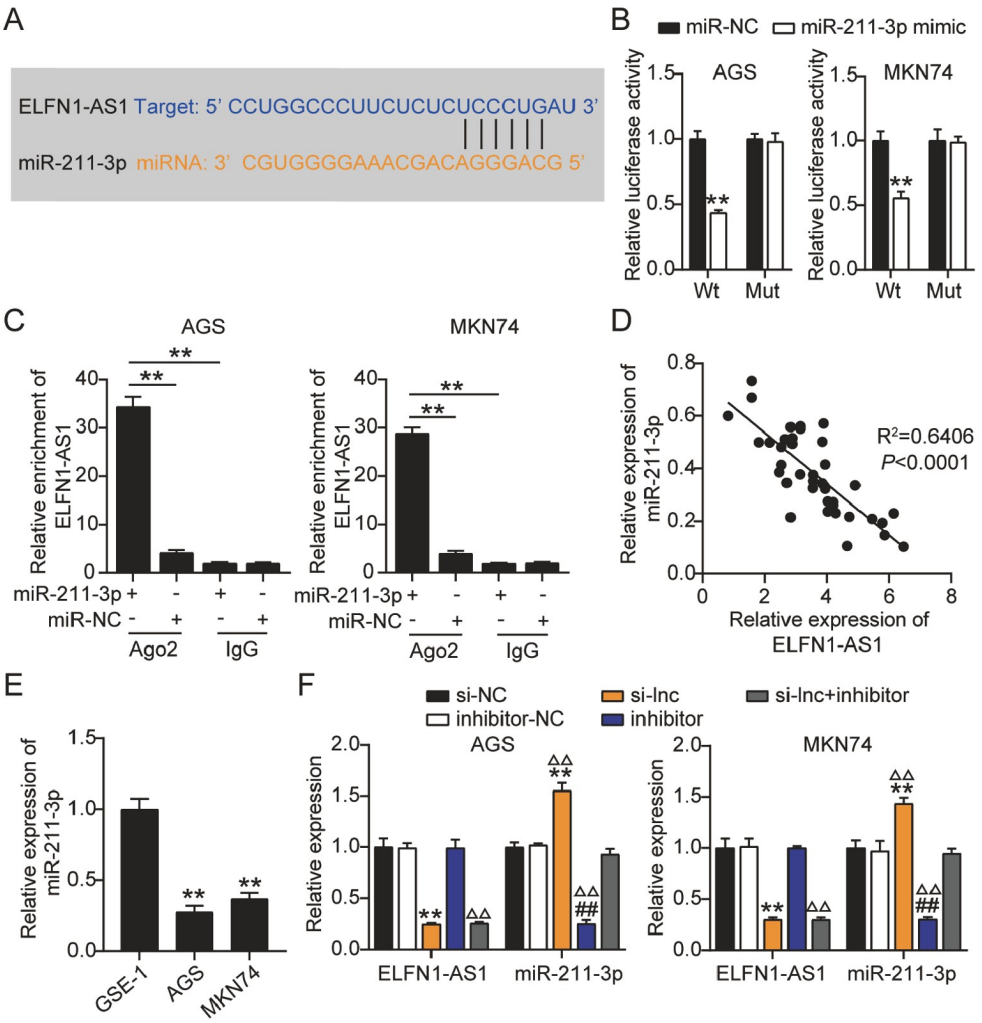

Figure 5. ELFN1-AS1 functions as a miR-211-3p sponge in GC cells (A) StarBase analysis predicting the binding sequences of miR-211-3p for ELFN1-AS1. (B) In AGS and MKN74 cells, luciferase activity was assessed by luciferase assay using wild-type or mutant ELFN1-AS1 and miR-211-3p mimic or mimics NC (miR-NC). (C) RIP analysis using Ago2 antibody to detect the enrichment of ELFN1-AS1 in AGS and MKN74 cell lines transfected with miR-211-3p mimics or miR-NC. (D) Pearson correlation between miR-211-3p and MKN74 in 40 GC tissues. (E) RT-qPCR analysis measuring miR-211-3p expression in AGS and MKN74 cells and GSE-1 cells. (F) AGS and MKN74 cells were transfected with si-lnc ELFN1-AS1#1 or miR-211-3p inhibitor and examined for their expression by real-time PCR. $^{**}P < 0.01$ vs miR-NC/anti-IgG; $^{\#\#}P < 0.01$ vs inhibitor-NC; $^{\Delta\Delta}P < 0.01$ vs si-lnc + inhibitor. NC, negative control; si-lnc, ELFN1-AS1; inhibitor, miR-211-3p inhibitor; and si-lnc + inhibitor, siRNA-ELFN1-AS1-AS1 + miR-211-3p inhibitor.

siRNA-ELFN1-AS1 and miR-211-3p inhibitor cotransfection on the migration, invasion, and EMT of GC cells was also evaluated. The reduced migratory capacity of GC cells due to *ELFN1-AS1* silencing was avoided by cotransfecting the cells with the miR-211-3p inhibitor (Figure 7A). Similarly, introducing the miR-211-3p inhibitor into *ELFN1-AS1*-silenced GC cells considerably reversed the inhibitory effects of si-ELFN1-AS1 on GC cell invasion and EMT (Figure 7B,C).

Additionally, OE-lnc and miR-211-3p mimics were cotransfected into GC cells to verify the above conclusions. Overexpression of ELFN1-AS1 downregulated miR-211-3p expression by 75%, which was reversed in both GC cell lines transfected with the miR-211-3p mimic. Moreover, examination of the biological function of GC cells revealed that ELFN1-AS1 overexpression promoted the proliferation, migration, and invasion of AGS and MKN74 cells and inhibited their apoptosis. Furthermore, the miR-211-3p mimic reversed the malignant behavior of ELFN1-AS1-overexpressing GC cells (Supplementary Figures S2 and S3).

MiR-211-3p targets TRIM29 and reduces its expression in GC cells

A miRNA degrades its target mRNA and reduces target gene expression, thereby contributing to the pathogenesis of neoplasia. Therefore, we performed TargetScan, which predicted that the 3′-UTR of TRIM29 contained putative binding sites for miR-211-3p (Figure 8A). This direct targeting relationship was verified by the luciferase reporter assay, which showed a decrease in luciferase activity in GC cells transfected with luciferase-TRIM29 3′-UTR-WT

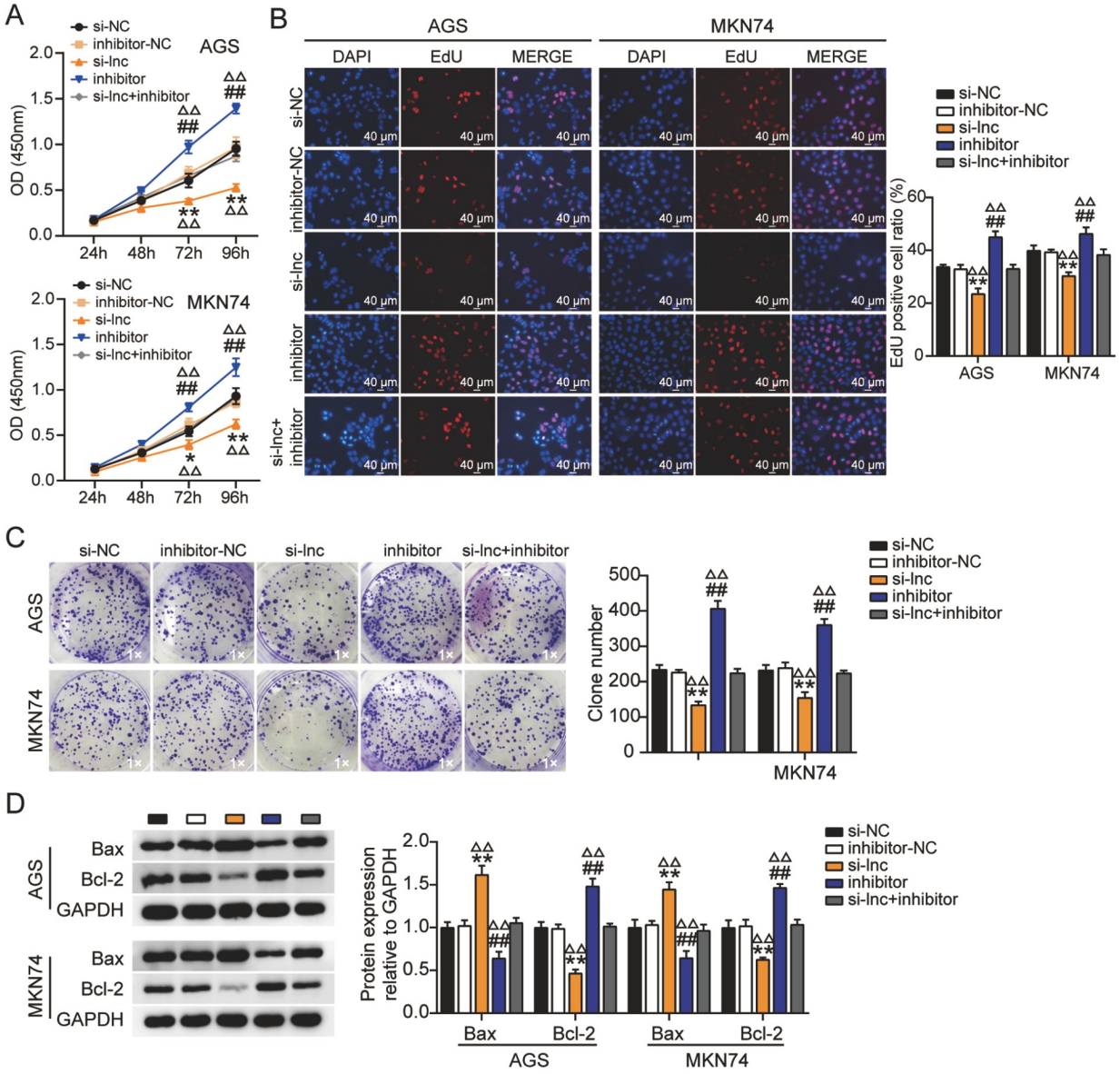

Figure 6. MiR-211-3p inhibitor alleviates the repressive effect of *ELFN1-AS1* silencing on proliferation of GC cells *in vitro* AGS and MKN74 cells were transfected with si-lnc NC, si-lnc, miR-211-3p inhibitor, and si-lnc + inhibitor. (A) CCK-8 cell proliferation assay. (B) EdU cell proliferation assay. (C) Colony formation assay. (D) Western blot analysis of Bax and Bcl-2 expressions. $^{**}P < 0.01$ vs si-NC; $^{\#\#}P < 0.01$ vs inhibitor-NC; $^{\Delta\Delta}P < 0.01$ vs si-lnc + inhibitor. NC, negative control; si-lnc, siRNA-ELFN1-AS1#1; inhibitor, miR-211-3p inhibitor; and si-lnc + inhibitor, siRNA-ELFN1-AS1#1 + miR-211-3p inhibitor.

and the miR-211-3p mimic (Figure 8B). RNA pull-down assay confirmed the direct binding relationship of miR-211-3p with TRIM29 in GC cells (Figure 8C). Next, RT-qPCR analysis was performed to compare TRIM29 expression in GC and normal tissues. In contrast to the low expression of miR-211-3p in GC tissues, TRIM29 was highly expressed (Figure 8D). Pearson's correlation analysis demonstrated that TRIM29 expression was negatively correlated with miR-211-3p expression (Figure 8E). TRIM29 expression was also higher in GC cells than in GSE-1 cells (Figure 8F). To further examine the specificity of this negative correlation, AGS and MKN74 cells were transfected with si-TRIM29, miR-211-3p inhibitor, or their NCs alone or in combination with si-TRIM29 and miR-211-3p inhibitor. Transient transfection of the miR-211-3p inhibitor increased TRIM29 expression in GC cells and restored TRIM29 expression in *TRIM29*-silenced GC cells (Figure 8G). Additionally, TRIM29 protein levels were reduced in *ELFN1-AS1*-silenced GC cells (Figure 8H). Overall, these findings suggest that miR-211-3p, which specifically targets TRIM29, is sponged by ELFN1-AS1.

miR-211-3p acts as a protumor factor by targeting TRIM29

We investigated whether miR-211-3p affects the malignant phenotypes of GC cells by targeting TRIM29. CCK8 assays revealed a low

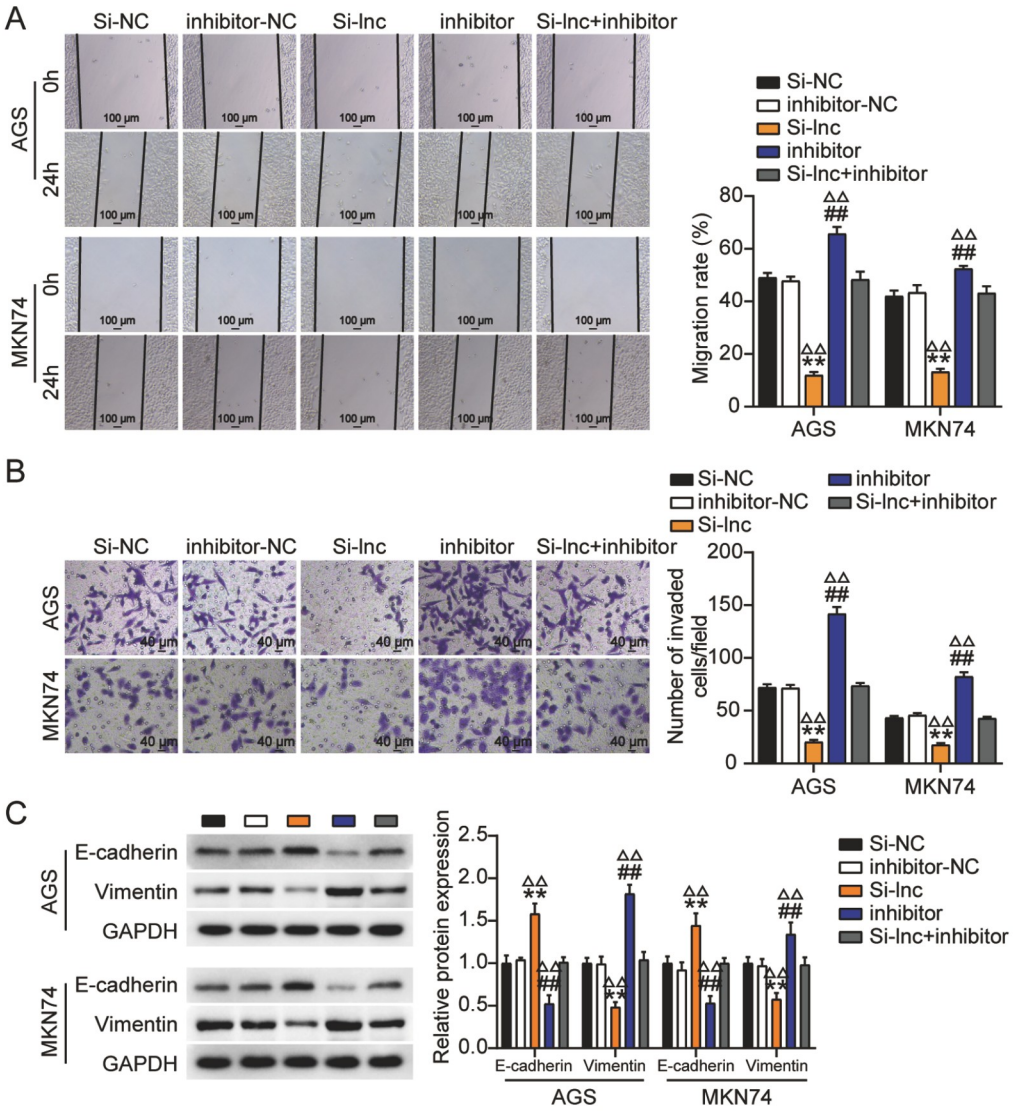

Figure 7. MiR-211-3p inhibitor alleviates the repressive effect of *ELFN1-AS1* silencing on the migration and invasion of GC cells *in vitro* AGS and MKN74 cells were transfected with si-lnc NC, si-lnc, miR-211-3p inhibitor, and si-lnc + inhibitor. (A) Wound healing assay of AGS and MKN74 cells. (B) Transwell invasion of AGS and MKN74 cells. (C) Western blot analysis of E-cadherin and vimentin expressions. $^{**}P < 0.01$ vs si-NC; $^{\#\#}P < 0.01$ vs inhibitor-NC; $^{\Delta\Delta}P < 0.01$ vs si-lnc + inhibitor. NC, negative control; si-lnc, siRNA- ELFN1-AS1#1; inhibitor, miR-211-3p inhibitor; and si-lnc + inhibitor, siRNA-ELFN1-AS1#1 + miR-211-3p inhibitor.

and high proliferative rate of cells transfected with si-TRIM29 and miR-211-3p inhibitor, respectively. Furthermore, *TRIM29* silencing reversed the effect of the miR-211-3p inhibitor on the proliferation of GC cells (Figure 9A). Similar results were obtained in EdU proliferation assays (Figure 9B). Additionally, the increased rate of colony formation in both cell lines caused by the miR-211-3p inhibitor was reversed by *TRIM29* knockdown (Figure 9C). In contrast to the effect of the miR-211-3p inhibitor on Bax and Bcl-2 expression, *TRIM29* knockdown enhanced Bax expression and reduced Bcl-2 expression. The levels of both apoptosis-related proteins in cells cotransfected with si-TRIM29 and miR-211-3p inhibitor were comparable to those in the NC group (Figure 9D). The higher migratory rates of GC cells after miR-211-3p inhibitor transfection were reversed by *TRIM29* knockdown, indicating that interaction with TRIM29 was essential for miR-211-3p to suppress GC cell migration (Figure 10A). Likewise, introducing si-TRIM29 into miR-211-3p-silenced GC cells substantially reversed the stimulatory effects of the miR-211-3p inhibitor on GC cell invasion and EMT (Figure 10B,C). These results suggest that miR-211-3p suppresses GC progression *in vitro* by targeting TRIM29.

Discussion

In the present study, using the GEPIA database, we found that ELFN1-AS1 was highly expressed in GC tissues and negatively correlated with the prognosis of GC patients, suggesting a significant involvement of ELFN1-AS1 in GC. Moreover, silencing of ELFN1-AS1 blocked the proliferation, migration, invasion, and EMT of GC cells and increased their apoptotic rate. Subsequent

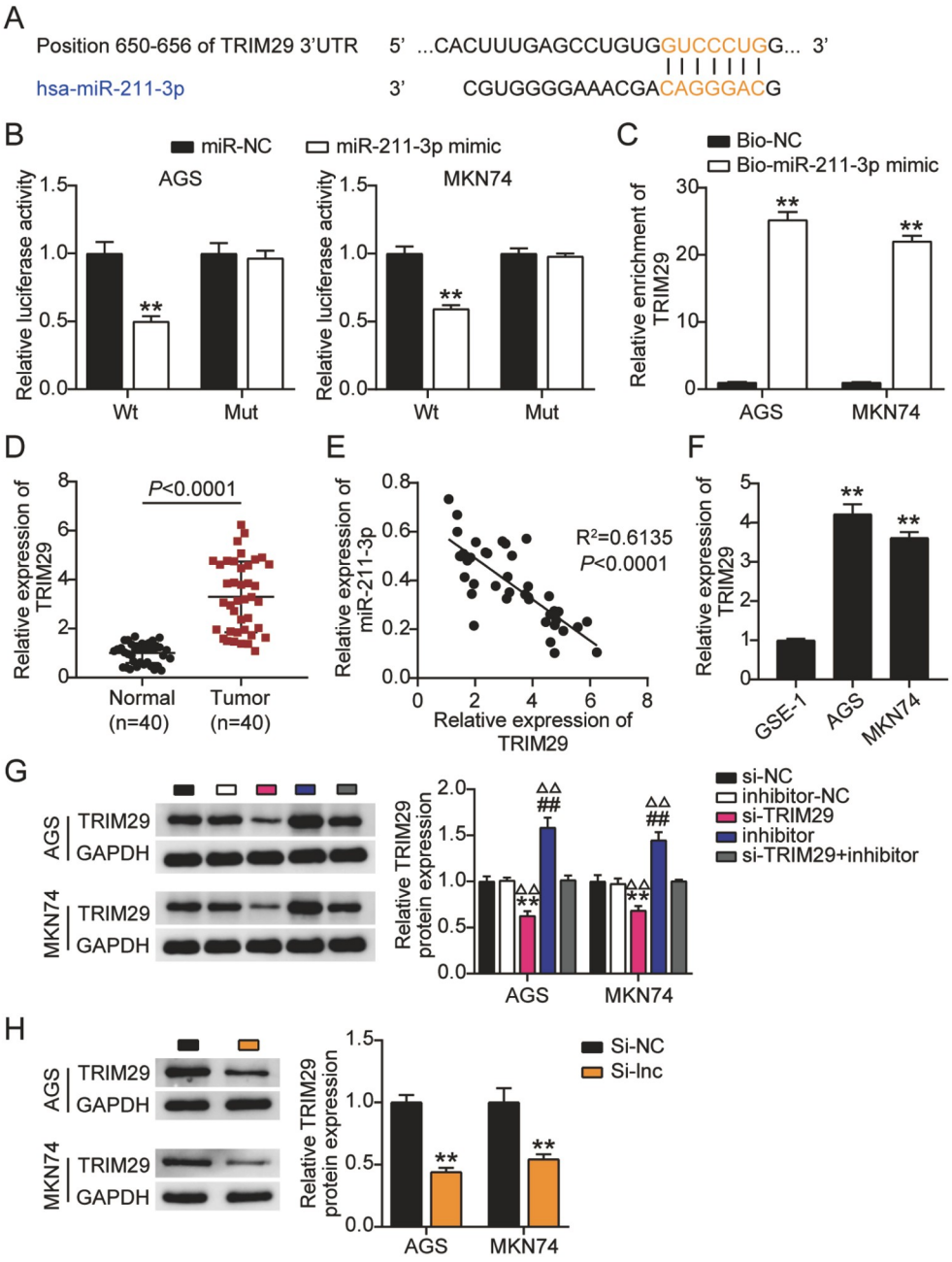

Figure 8. MiR-211-3p targets TRIM29 and lessens its expression in GC cells (A) StarBase analysis predicting the predicted binding sequences of TRIM29 and miR-211-3p. (B) A dual luciferase assay was performed in GC cells cotransfected with TRIM29 3′UTR-WT or TRIM29 3′UTR-Mut plasmids and NC mimics or miR-211-3p mimic in AGS and MKN74 cells. The luciferase activities were examined using a luciferase assay kit. $^{**}P<0.01$ vs miR-NC. (C) The enrichment of TRIM29 and miR-211-3p by RNA pull-down assay. $^{**}P<0.001$ vs Bio-NC. (D) RT-qPCR detection of TRIM29 expression in 40 GC tissues and 40 normal tissues. (E) The correlation between the relative expression level of miR-211-3p targets TRIM29. (F) RT-qPCR detection of TRIM29 expression in GC cells (AGS and MKN74 cells) and normal cells (GSE-1). $^{**}P<0.01$ vs GSE-1. (G) Western blot analysis of TRIM29 protein expression in GC cells transfected with si-NC, inhibitor-NC, si-TRIM29 and si-TRIM29 + inhibitor. $^{**}P<0.01$ vs si-NC; $^{\#\#}P<0.01$ vs inhibitor-NC; $^{\Delta\Delta}P<0.01$ vs si-TRIM29 + inhibitor. (H) Western blot analysisTRIM29 protein expression in GC cells transfected with si-NC and si-lnc. $^{**}P<0.01$ vs si-NC. NC, negative control; WT, wild-type; Mut, mutant; si-TRIM29, siRNA-TRIM29; inhibitor, miR-211-3p inhibitor; si-TRIM29 + inhibitor, siRNA-TRIM29 + miR-211-3p inhibitor; and si-lnc, siRNA-ELFN1-AS1#1.

mechanistic assays showed that ELFN1-AS1 sequestered miR-211-3p, thereby increasing TRIM29 expression, which in turn promoted GC progression. The observed negative association between miR-211-3p and ELFN1-AS1/TRIM29 expressions in GC tissues provided further evidence for the interactions between ELFN1-AS1, miR-211-3p, and TRIM29.

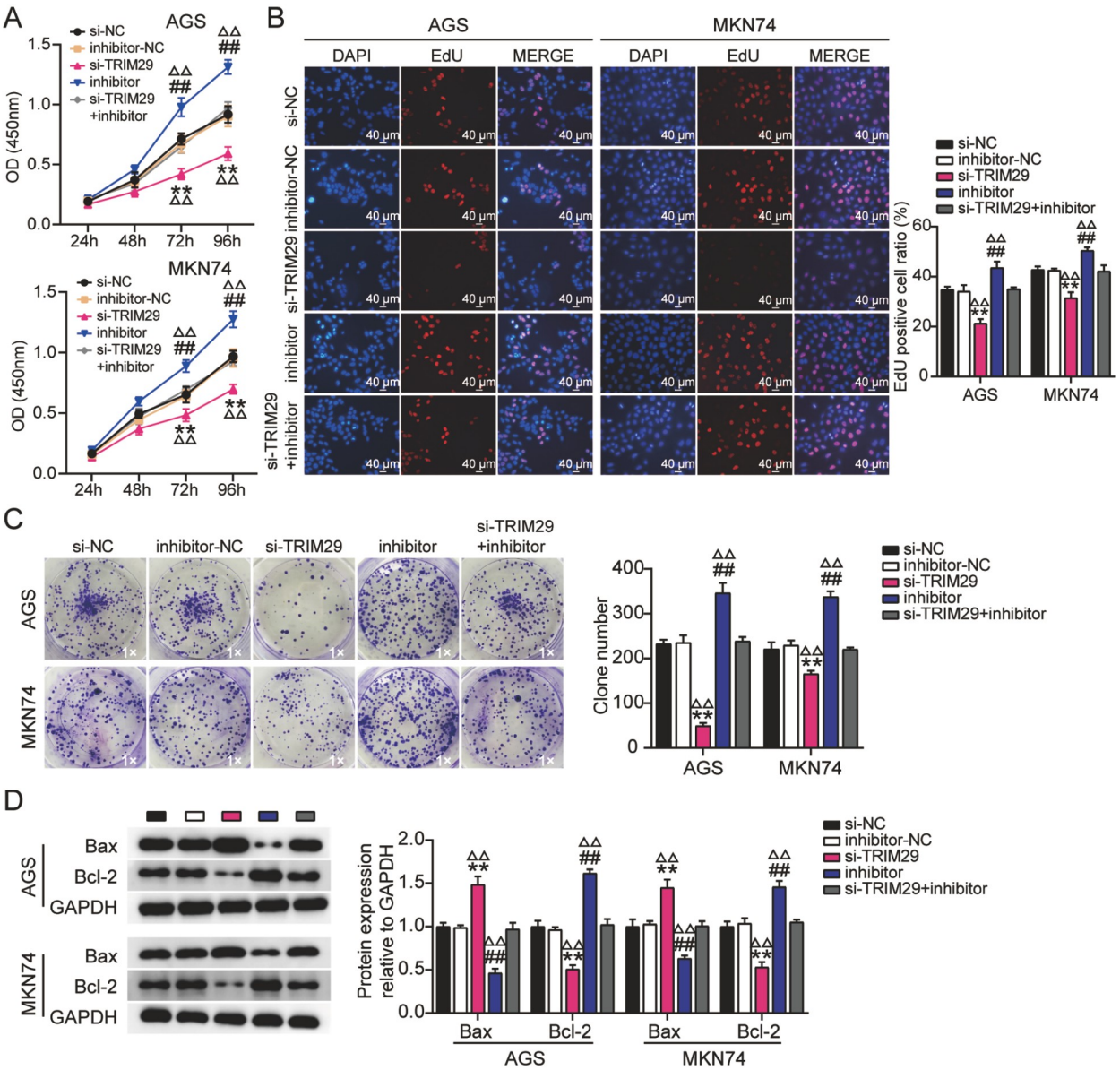

Figure 9. MiR-211-3p impairs GC cell proliferation and triggers apoptosis by targeting TRIM29 AGS and MKN74 cells were transfected with NC, si-TRIM29, miR-211-3p inhibitor, and si-TRIM29 + miR-211-3p inhibitor. (A) CCK8 assays were used to assess cell viability. (B) EdU assay was used to detect cell proliferation. (C) *In vitro* colony formation assay confirmed the *in vivo* observation. (D) Western blot analysis of Bax and Bcl-2 expressions. $^{**}P < 0.01$ vs si-NC; $^{\#\#}P < 0.01$ vs inhibitor-NC; $^{\Delta\Delta}P < 0.01$ vs si-TRIM29 + inhibitor. NC, negative control; si-TRIM29, siRNA-TRIM29; inhibitor, miR-211-3p inhibitor; and si-TRIM29 + inhibitor, siRNA-TRIM29 + miR-211-3p inhibitor.

The important regulatory role of lncRNAs has been identified in various pathological conditions, such as cancers [22]. As mentioned in the introduction, increasing evidence links GC progression to lncRNA dysregulation. Our results are consistent with previous studies that reported a protumorigenic role of ELFN1-AS1 in various cancers [9–13]. We also found that ELFN1-AS1 was upregulated in GC tissues (and cell lines) and negatively associated with the clinical outcomes of GC patients. In line with previous reports, we found that *ELFN1-AS1* silencing can attenuate the malignancy of GC cells and trigger their apoptosis. Interestingly, the EMT pathway was involved in the pathogenesis of GC. Our results indicated that ELFN1-AS1 may promote GC cell migration and invasion by inducing EMT, as we observed increased E-cadherin and decreased vimentin in ELFN1-AS1-knockdown GC cells. Our findings are consistent with a recent pancreatic cancer study, in which ELFN1-AS1 was found to be involved in cancer progression by promoting EMT [13]. EMT is a critical step in tumorigenesis that promotes cancer cell metastasis and stemness. EMT downregulates the expressions of epithelial-specific markers (such as cytokeratins and E-cadherin) and increases the expressions of mesenchymal markers (such as fibronectin, N-cadherin, and vimentin) [23]. To the best of our knowledge, the present study is the first to

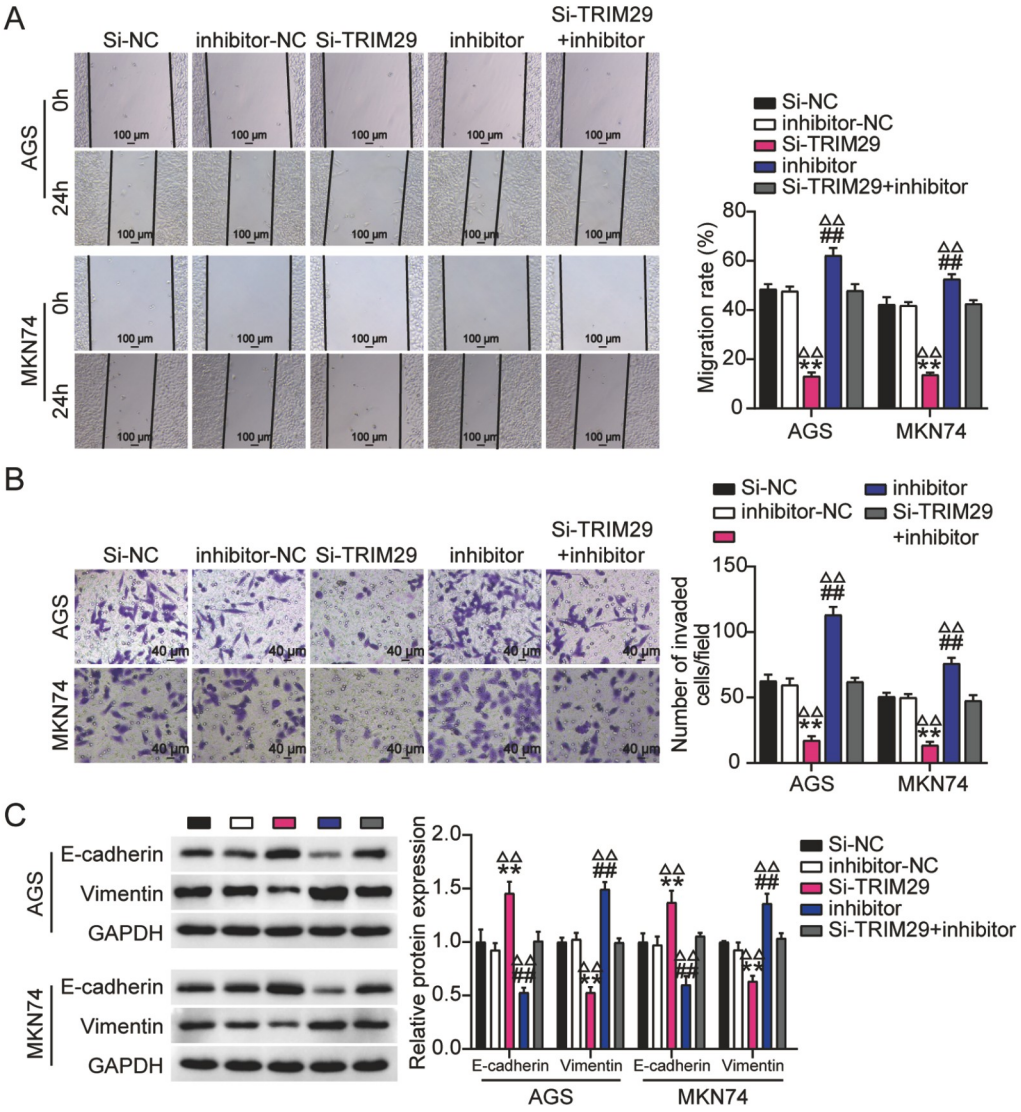

Figure 10. MiR-211-3p impairs GC cell migration and invasion by targeting TRIM29 AGS and MKN74 cells were transfected with NC, si-TRIM29, miR-211-3p inhibitor, and si-TRIM29 + miR-211-3p inhibitor. (A) Cell migration was detected by wound healing assay at 24 h posttransfection ($n = 3$). (B) Cell invasion was analyzed by Transwell invasion assay ($n = 3$). (C) Evaluation of E-cadherin and vimentin levels by western blot analysis. $^{**}P < 0.01$ vs si-NC; $^{\#\#}P < 0.01$ vs inhibitor-NC; $^{\Delta\Delta}P < 0.01$ vs si-TRIM29 + inhibitor. NC, negative control; si-TRIM29, siRNA-TRIM29; inhibitor, miR-211-3p inhibitor; and si-TRIM29 + inhibitor, siRNA-TRIM29 + miR-211-3p inhibitor.

demonstrate that ELFN1-AS1 plays a role in GC.

ELFN1-AS1 was found to be predominantly localized in the cytoplasm, indicating its ceRNA activity in GC. Our bioinformatics and RT-qPCR analyses indicated that miR-211-3p is a sensitive miRNA, which was further analyzed. miR-211-3p has been found to possess anticarcinogenic potential in various cancers [24–26]. However, its significance in GC has been overlooked. We observed that transfection of GC cells with miR-211-3p inhibitor promoted their proliferation, migration, invasion, and EMT but inhibited their apoptosis. Thus, our findings are consistent with previous research demonstrating that miR-211-3p has anticancer properties [24–26]. The downregulation of miR-211-3p in GC tissues and its negative correlation with ELFN1-AS1 further suggested the involvement of miR-211-3p in the ceRNA activity of ELFN1-AS1.

According to the bioinformatics analysis, TRIM29 was characterized as another member of the competitive platform for miR-211-3p and ELFN1-AS1 because of its miRNA/mRNA complementarity. Its capacity to assemble homo or heterodimers enables it to participate in nucleic acid binding as an effector or scaffold protein, thereby influencing genomic stability. Therefore, its dysregulation affects many broad and diverse cellular functions, particularly those in cancer. The role of TRIM29 depends on the cell and tissue type [27–29]. However, its cellular functions in GC remain unclear. We found that TRIM29 was upregulated in GC, and patients with high TRIM29 expression had a worse prognosis, indicating a tumor-promoting role of TRIM29 in GC. Additionally, silencing of *TRIM29* in GC cells suppressed the malignancy of GC cells, further confirming its oncogenic potential. More importantly, *TRIM29* silencing reversed

the miR-211-3p inhibitor-mediated effects on GC cells. The negative TRIM29 mRNA-miR-211-3p association further reinforced their interaction in GC. In conclusion, we found that ELFN1-AS1 promotes GC progression by regulating the miR-211-3p/TRIM29 axis. Thus, it may be a reliable prognostic marker and treatment target for GC.

In summary, bioinformatics analysis revealed that ELFN1-AS1 and TRIM29 are highly expressed in GC. Knockdown of *ELFN1-AS1* inhibits GC progression *in vitro*. Further mechanistic analyses revealed that ELFN1-AS1 functions as a ceRNA to sponge miR-211-3p and subsequently stimulates TRIM29 expression, thereby promoting GC progression. Our study increases the scope for discovering promising biomarkers and therapeutic targets for GC.

Supplementary Data

Supplementary data is available at *Acta Biochimica et Biophysica Sinica* online.

Funding

This work was supported by the grants from the Leading Talents Project of Central Plains Thousand Talents Program (No. 204200510023) and the Provincial and Ministerial Joint Project of Henan Medical Science and Technology Program (No. SB201901101).

Conflict of Interest

The authors declare that they have no conflict of interest.

References

1. Sung H, Ferlay J, Siegel RL, Laversanne M, Soerjomataram I, Jemal A, Bray F. Global cancer statistics 2020: GLOBOCAN estimates of incidence and mortality worldwide for 36 cancers in 185 countries. *CA Cancer J Clin* 2021, 71: 209–249
2. Song Z, Wu Y, Yang J, Yang D, Fang X. Progress in the treatment of advanced gastric cancer. *Tumour Biol* 2017, 39: 101042831771462
3. Karimi P, Islami F, Anandasabapathy S, Freedman ND, Kamangar F. Gastric cancer: descriptive epidemiology, risk factors, screening, and prevention. *Cancer Epidemiol Biomarkers Preve* 2014, 23: 700–713
4. Wei L, Sun J, Zhang N, Zheng Y, Wang X, Lv L, Liu J, *et al.* Noncoding RNAs in gastric cancer: implications for drug resistance. *Mol Cancer* 2020, 19: 62
5. Zhang G, Li S, Lu J, Ge Y, Wang Q, Ma G, Zhao Q, *et al.* LncRNA MT1JP functions as a ceRNA in regulating FBXW7 through competitively binding to miR-92a-3p in gastric cancer. *Mol Cancer* 2018, 17: 87
6. Feng H, Liu X. Interaction between ACOT7 and LncRNA NMRAL2P via methylation regulates gastric cancer progression. *Yonsei Med J* 2020, 61: 471–481
7. Deng W, Wang J, Zhang J, Cai J, Bai Z, Zhang Z. TET2 regulates LncRNA-ANRIL expression and inhibits the growth of human gastric cancer cells. *IUBMB Life* 2016, 68: 355–364
8. Deng W, Zhang Y, Cai J, Zhang J, Liu X, Yin J, Bai Z, *et al.* LncRNA-ANRIL promotes gastric cancer progression by enhancing NF-kB signaling. *Exp Biol Med (Maywood)* 2019, 244: 953–959
9. Zhang C, Lian H, Xie L, Yin N, Cui Y. LncRNA ELFN1-AS1 promotes esophageal cancer progression by up-regulating GFPT1 via sponging miR-183-3p. *Biol Chem* 2020, 401: 1053–1061
10. Lei R, Feng L, Hong D. ELFN1-AS1 accelerates the proliferation and migration of colorectal cancer via regulation of miR-4644/TRIM44 axis. *Cancer Biomark* 2020, 27: 433–443
11. Jie Y, Ye L, Chen H, Yu X, Cai L, He W, Fu Y. ELFN1-AS1 accelerates cell proliferation, invasion and migration via regulating miR-497-3p/CLDN4 axis in ovarian cancer. *Bioengineered* 2020, 11: 872–882
12. Dong L, Ding C, Zheng T, Pu Y, Liu J, Zhang W, Xue F, *et al.* Extracellular vesicles from human umbilical cord mesenchymal stem cells treated with siRNA against ELFN1-AS1 suppress colon adenocarcinoma proliferation and migration. *Am J Transl Res* 2019, 11: 6989–6999
13. Ma G, Li G, Gou A, Xiao Z, Xu Y, Song S, Guo K, *et al.* Long non-coding RNA ELFN1-AS1 in the pathogenesis of pancreatic cancer. *Ann Transl Med* 2021, 9: 877
14. Hatakeyama S. TRIM proteins and cancer. *Nat Rev Cancer* 2011, 11: 792–804
15. Xu M, Hu J, Zhou B, Zhong Y, Lin N, Xu R. TRIM29 prevents hepatocellular carcinoma progression by inhibiting Wnt/β-catenin signaling pathway. *Acta Biochim Biophys Sin* 2019, 51: 68–77
16. Xu W, Chen B, Ke D, Chen X. TRIM29 mediates lung squamous cell carcinoma cell metastasis by regulating autophagic degradation of E-cadherin. *Aging* 2020, 12: 13488–13501
17. Wang C, Zhou Y, Chen B, Yuan W, Huang J. Prognostic value of tripartite motif containing 29 expression in patients with gastric cancer following surgical resection. *Oncol Lett* 2018, 15: 5792–15798
18. Qiu F, Xiong JP, Deng J, Xiang XJ. TRIM29 functions as an oncogene in gastric cancer and is regulated by miR-185. *Int J Clin Exp Pathol* 2015, 8: 5053–5061
19. Shan Y, Ma J, Pan Y, Hu J, Liu B, Jia L. LncRNA SNHG7 sponges miR-216b to promote proliferation and liver metastasis of colorectal cancer through upregulating GALNT1. *Cell Death Dis* 2018, 9: 722
20. Tian F, Wang J, Zhang Z, Yang J. LncRNA SNHG7/miR-34a-5p/SYVN1 axis plays a vital role in proliferation, apoptosis and autophagy in osteoarthritis. *Biol Res* 2020, 53: 9
21. Sobierajska K, Ciszewski WM, Macierzynska-Piotrowska E, Klopocka W, Przygodzka P, Karakula M, Pestka K, *et al.* The new model of snail expression regulation: the role of MRTFs in fast and slow endothelial-mesenchymal transition. *Int J Mol Sci* 2020, 21: 5875
22. Bhan A, Soleimani M, Mandal SS. Long noncoding RNA and cancer: a new paradigm. *Cancer Res* 2017, 77: 3965–3981
23. Ribatti D, Tamma R, Annese T. Epithelial-mesenchymal transition in cancer: a historical overview. *Transl Oncol* 2020, 13: 100773
24. Ma XR, Xu YL, Qian J, Wang Y. Long non-coding RNA SNHG15 accelerates the progression of non-small cell lung cancer by absorbing miR-211-3p. *Eur Rev Med Pharmacol Sci* 2019, 23: 1536–1544
25. Kong Q, Qiu M. Long noncoding RNA SNHG15 promotes human breast cancer proliferation, migration and invasion by sponging miR-211-3p. *Biochem Biophys Res Commun* 2018, 495: 1594–1600
26. Feng R, Li Z, Wang X, Ge G, Jia Y, Wu D, Ji Y, *et al.* Silenced lncRNA SNHG14 restrains the biological behaviors of bladder cancer cells via regulating microRNA-211-3p/ESM1 axis. *Cancer Cell Int* 2021, 21: 67
27. Sun J, Yan J, Qiao HY, Zhao FY, Li C, Jiang JY, Liu BQ, *et al.* Loss of TRIM29 suppresses cancer stem cell-like characteristics of PDACs via accelerating ISG15 degradation. *Oncogene* 2020, 39: 546–559
28. Hao L, Wang JM, Liu BQ, Yan J, Li C, Jiang JY, Zhao FY, *et al.* m6A-YTHDF1-mediated TRIM29 upregulation facilitates the stem cell-like phenotype of cisplatin-resistant ovarian cancer cells. *Biochim Biophys Acta* 2021, 1868: 118878
29. Sun J, Zhang T, Cheng M, Hong L, Zhang C, Xie M, Sun P, *et al.* RETRACTED ARTICLE: TRIM29 facilitates the epithelial-to-mesenchymal transition and the progression of colorectal cancer via the activation of the Wnt/β-catenin signaling pathway. *J Exp Clin Cancer Res* 2019, 38: 104